4688 *Macromolecules* **2010**, *43*, 4688–4697
DOI: 10.1021/ma1006073

Macromolecules
ARTICLE

Rapid Radical Degradation Test of Polyaromatic Fuel Cell Membranes by Electron Paramagnetic Resonance

Barbara Vogel, Herbert Dilger, and Emil Roduner*

Institute of Physical Chemistry, University of Stuttgart, Pfaffenwaldring 55, 70569 Stuttgart, Germany

Received March 19, 2010; Revised Manuscript Received April 20, 2010

ABSTRACT: A novel setup based on electron paramagnetic resonance is used for the investigation of the hydroxyl radical driven degradation on contact of gaseous hydrogen peroxide with sulfonated polyetherketones. This method is more sensitive than mass loss investigations and allows obtaining results 300 times faster and with higher accuracy. Furthermore, it reveals detailed information about the character and amount of paramagnetic intermediates formed during degradation. The spectra are composed of three signals which are attributed to sulfonyl, phenyl, and phenoxy type radicals. Drying the membranes in the absence of hydrogen peroxide leads to internal tension of the ionomer material and to bond breakage, and therefore also to a small amount of radical defects. The presence of the peroxide at first leads to a linear increase in radical concentration. The kinetics is compatible with a dissociative Langmuir type chemisorption process. With progressing degradation time, a steady state is reached due to saturation of the surface and to radical termination. It is accompanied by cross-linking the polymer and increasing its brittleness. The surface layer then breaks off and leaves the sample in pieces (peel-off effect), providing a significant mass loss at random times. Between the two studied commercial membranes, sulfonated poly(phthalazinone ether ketone) was found to be more inert toward hydroxyl radicals than sulfonated poly(ether ether ketone).

1. Introduction

After 40 years of development of polymer electrolyte membrane fuel cells (PEMFCs), high costs, the limited efficiency of the catalysts, and the insufficient stability of the membranes are still the main points of concern. Membranes face very harsh conditions in the working fuel cell, such as locally very low pH,[1] mechanical stress because of inhomogeneous temperature, gas and humidity distribution as well as radical attack by side products of the electrocatalytic reactions. Hydrogen atoms ($^{\bullet}$H), hydroxyl ($^{\bullet}$OH) and hydroperoxyl ($^{\bullet}$OOH) radicals exist in relatively low concentrations[2] and are assumed to be responsible for chemical degradation. Methods for quantitative investigation of these processes are currently being developed.

In situ measurements in working fuel cells provide an overview over the relevant steps of degradation but only very few allow distinguishing individual processes.[3] To simplify the complex situation it seems promising to study reactions of individual components, especially radical attack on bare membranes. Conventionally, this is done using hydrogen peroxide and produce its radical cleavage product, $^{\bullet}$OH. Radicals were reported to be formed in a zero-order reaction of H_2O_2 on solid surfaces (polymer membrane, quartz glass tube) at temperatures higher than 60 °C.[4]

So far, degradation was studied using several quantitative methods, mostly by exposure to hot, liquid hydroperoxide solution,[5] but it was also shown that dry membrane conditions represent much harsher conditions regarding oxidative chemical degradation with hydroperoxide.[6] One of the methods involves the measurement of the mass loss of membranes, which is very time-consuming, and even special overnight drying procedures cannot fully avoid significant weighing errors.[7] Other work involved detailed chemical product analysis.[8] Electron paramagnetic resonance (EPR) is a well-known method allowing the identification of paramagnetic intermediates, also in the context of fuel cell membranes.[9] In investigations of ionomers it reveals the sites of preferential radical attack. Spin trap EPR with an in situ fuel cell in the resonator of the spectrometer has been used to demonstrate radical formation, including $^{\bullet}$OH, in a running fuel cell.[2,3] Using a double resonator setup, EPR permits spin quantification,[10] which allows the determination of the radical concentration and leads to a time-resolved picture of radical formation and termination depending on measurement conditions and material structure. On this basis, strategies to extend the stability of membranes can be developed. So far, most of the work concentrated on perfluorinated ionomers.

Here we report a rapid EPR test for fast and quantitative in situ monitoring of radical defect formation on two nonfluorinated sulfonated hydrocarbon membranes under the influence of hydrogen peroxide vapor at variable temperature and humidity. It simulates the radical driven membrane degradation by $^{\bullet}$OH radicals in a working fuel cell. The membrane samples are conditioned before exposing them to gaseous hydrogen peroxide by bubbling nitrogen through a 3% aqueous solution at 5 °C. Relative to air the nitrogen atmosphere increases the lifetime of free and membrane trapped radicals and conserves their nature. In air, carbon-centered radicals are known to be trapped by dioxygen under the formation of peroxy radicals. The present study leads to an unexpected insight into the mass-loss mechanism.

2. Experimental Section

2.1. Setup. The central element of the degradation setup shown in Scheme 1 is a double-walled quartz glass cylinder, the outer tube (inner diameter 8 mm) of which is used for heating by a flow of temperature-controlled nitrogen. The inner tube (inner diameter 4 mm) has a small nib to hold the polymer sample stripes in place. Water vapor or hydrogen peroxide vapor is fed in from the top via a second, continuous nitrogen

*Corresponding author. E-mail: e.roduner@ipc.uni-stuttgart.de.

 Published on Web 04/29/2010 © 2010 American Chemical Society

Scheme 1. Schematic Sketch of Rapid Test Setup

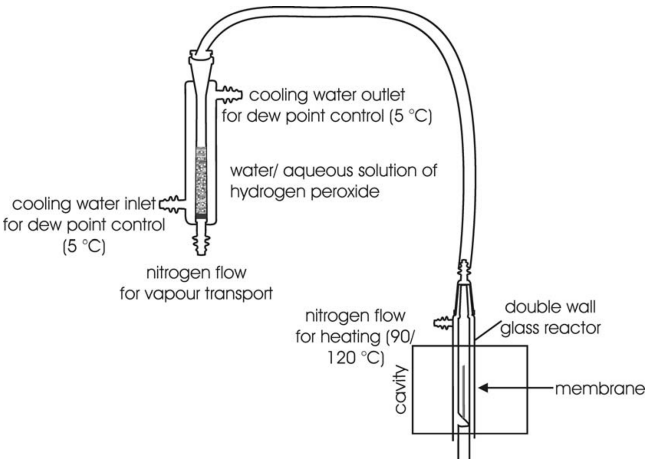

flow. Condensed liquid drips out at the outlet, and gaseous degradation products escape. Temperature inside the reaction chamber was measured using a sensor placed in the gas flow close to the sample.

Humidification is set by a humidifier that is controlled by a thermostat which cools the liquid (water or hydrogen peroxide) in the reservoir to 5 °C. A nitrogen flow of 0.4 $L \cdot min^{-1}$ saturates to maximum humidity (dew point: 5 °C) while passing the humidifier. This gas flow enters the reactor, where it is heated up to 65 or 80 °C, corresponding to 3.5 and 1.8% relative humidity (r.h.), respectively. At this low humidity water does not condense in the reaction chamber. This is essential for EPR spectroscopy, because water dissipates microwaves strongly, thereby reducing the sensitivity of the experiments.

For all measurements the membranes were first conditioned by passing the nitrogen through plain water. After a few hours, the treatment was switched to hydrogen peroxide solution.

2.2. Investigated Materials. Two polyaromatic membranes, s-PPEK and s-PEEK from FuMaTech, were investigated in the present work. Complementary measurements were carried out with two additional, related materials to support the assignment of the observed radicals. Table 1 shows the chemical composition and physical characteristics of the samples. Following the recommendation in the data sheets[11] both samples were conditioned in 10 mL of 0.5 M sulfuric acid per 10 mg polymer at 80 °C. After 3 h they were taken out, rinsed with water and stored in demineralized water at room temperature.

When the samples are treated with hydrogen peroxide solution (30%, Perhydrol p.a. from Merck, diluted to 3 wt % with doubly distilled water) at 65 or 80 °C for more than 5 h, they became darker in color; the yellow P 730 turns brown, while the brown E 730 darkens.

2.3. Polymer Analysis. Although the method was developed to monitor membrane degradation more rapidly than by mass loss, the weight of all samples was checked after different periods of time. To identify molecular changes on the membrane different analytical methods were applied. For distinction between main chain attack and side chain cleavage (Scheme 3), measurement of the equivalent weight and elemental analysis were used.

2.3.1. Mass Loss and Equivalent Weight Measurements. To get a quick overview over mass loss dependence on degradation time, all fully proton exchanged samples were dried in an air conditioned room (23 °C dew point, 30% r.h.) and weighed before and after the experiment using a Sartorius E 214S balance. The samples (~4 mm × 50 mm) had typically a mass of 10 mg. Mass losses higher than 0.2 mg are reliably detectable.

The equivalent weight (EW), a common and easily measurable characteristic of membrane samples, is given in grams polymer per mol of sulfonic acid groups. It influences the degree of water

Table 1. Chemical Composition and Physical Characteristics of the Samples

Polymer type	Appearance	EW ($g \cdot mol^{-1}$) and thickness (μm) (literature [11]/ measured)	Molecular weight, glass transition temperature and chemical structure
s-PEEK sulfonated polyetheretherketone E 730 [12]	brownish transparent, flat	700/820 and 30/30	>50000 g/mol, T_g=150-160 °C 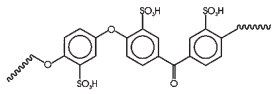
s-PPEK sulfonated polyphthalazinone etherketone P 730 [12]	yellowish transparent, flat	700/680 and 30/30	>90000 g/mol, T_g=220-240 °C 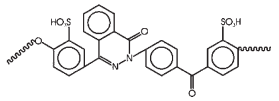
PEEK	white film of different thicknesses	--- and 20-100	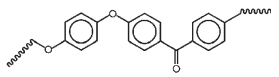
PSU	yellowish transparent	--- and 50	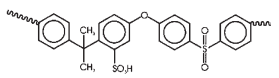

uptake and swelling of fuel cell membranes. Furthermore, it changes significantly when sulfonic acid groups are cleaved off or blocked by metal ions during the preparation procedure or in ionically cross-linked materials. Because of this blocking one distinguishes between the so-called TEW (total EW, all sulfonic acid groups) and the AEW (available EW, only free, protonated sulfonic acid groups).

For averaging out sample inhomogeneity, all investigations were performed on three membrane pieces following instructions in literature.[13] The EW was measured by titration of the membrane with sodium hydroxide solution and calculated using eq 1:

$$\mathrm{EW} = \frac{\text{dry weight of membrane [g]}}{\text{added volume (NaOH) [L]} \times \text{concentration (NaOH) [mol} \cdot \text{L}^{-1}]} \quad (1)$$

The end point at pH = 7 was determined using a pH sensitive electrode.

2.3.2. X-Band EPR. All investigations were performed in a double resonator of the Bruker EMX 10127 X-band spectrometer at 1 G modulation amplitude. The microwave power was varied (0.1, 1, or 4 mW, and 100 mW for special measurements at high power) based on the conditions in the cavity. An ultramarine blue sample of known spin concentration (3.0×10^{16} spins cm^{-1}) was placed in one of the resonators and measured as a standard simultaneously with the samples.

2.3.3. Data Analysis. For handling the high data rate the C++ based data analysis package "Root"[14] and its MINUIT minimization library were adapted and used for automatic fitting of Lorentzian functions and area calculation of EPR lines. For the

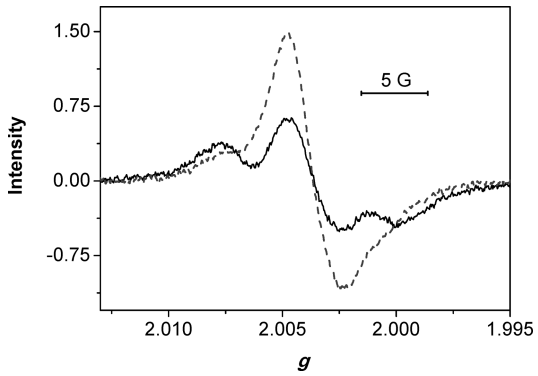

Figure 1. EPR signal of s-PEEK (E 730) after 15 h hydrogen peroxide treatment at 80 °C measured at 4 mW (broken line) and 100 mW (full line) microwave power.

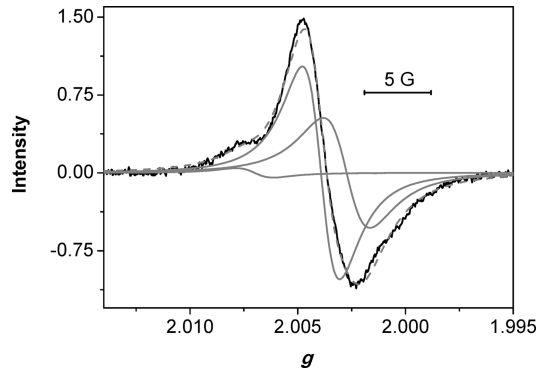

Figure 2. 4 mW spectrum obtained with s-PEEK (E 730) from Figure 1 (black), with fitted lines of three species (gray, solid line) and sum of fitted lines (gray, dashed line).

given signal-to-noise ratio fitting Gaussian line profiles did not lead to significant improvements of the fits.

Comparing areas of sample and reference spectra with each other and dividing by the membrane mass permit the calculation of the radical concentration in the sample. Origin 8.0[15] was used to fit the increase of radical concentrations with time.

3. Results and Discussion

3.1. Type and Origin of the Signals. *3.1.1. Signal Characteristics.* Figure 1 shows the EPR signal of s-PEEK (E 730) after 17 h of hydrogen peroxide treatment. It is stable and remains detectable in inert atmosphere for more than 1 week at −70 °C and for more than 100 h at +80 °C. With its shoulder on the left and the broad negative part of the signal it is asymmetric but does not have the typical anisotropic powder pattern line shape. This suggests the signal represents a superposition of different species.

In such a situation the presence of different species can often be distinguished based on their different relaxation times. Therefore, various microwave powers were applied, as demonstrated in Figure 1 for the example of E 730 (s-PEEK). The strongest saturation effect is shown by the center line, because its intensity decreases with increasing microwave power. The other two lines change their intensity only slightly, which means they are in the saturation region as well at 100 mW, but the saturation is weaker. Because of the different saturation behavior it is concluded that the EPR spectrum represents a superposition of three coexisting radical species.

The overlap of lines impedes the determination of *g* values directly from the graph. Therefore, a set of the three Lorentzian functions was fitted to the spectra (Figure 2) to obtain *g* values, line widths and areas from the parameter output.

3.1.2. Comparison of the Membranes. Figure 3 shows the EPR spectra of s-PEEK (E 730) and s-PPEK (P 730) after around 20 h of hydrogen peroxide treatment at 80 °C. Both signals are superpositions of three lines, but their intensity ratio is different for s-PEEK (E 730) and s-PPEK (P 730).

To exclude any saturation effects the fitting of the Lorentzian functions was to the spectra obtained at 0.1 mW. The *g* values are roughly equal for the two membranes (Table 2). It is therefore concluded that both membranes degrade via the same intermediates and mechanisms, which might have been expected as their chemical structure is similar. The isotropic nature and low line width of the signals indicates effective averaging of *g* anisotropies as a consequence of high chain mobility in the polymer at 80 °C. At room temperature, the spectra of, e.g., phenoxyl type radicals are far broader and show resolved components of the *g* tensor.[9,16]

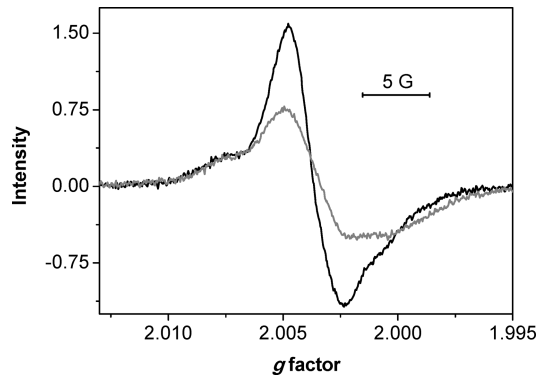

Figure 3. EPR spectra of s-PEEK (E 730, black) and s-PPEK (P 730, gray) after 18 h hydrogen peroxide treatment at 80 °C measured at 4 mW.

Table 2. Fit Results: *g* Values and Line Widths for s-PEEK (E 730) and s-PPEK (P 730)

	parameter	signal 1	signal 2	signal 3	errors
s-PEEK	*g* value	2.0016	2.0034	2.0071	±0.0001
	line width (G)	3.4	5.2	6.2	±0.1
s-PEKH	*g* value	2.0016	2.0038	2.0062	±0.0001
	line width (G)	3.4	6.9	7.6	±0.1

The two membrane types deviate in the ratio of ether to ketone groups, the EW value and most of all the phtalazinone bridge, which is only present in P 730 (s-PPEK).[12] Membranes with and without phtalazinone show the same signals, so the phtalazinone element does not form distinguishable EPR active products under the influence of hydrogen peroxide vapor and does probably not take part in the radical degradation mechanism. It has to be investigated whether differences in signal intensities can be directly correlated to differences in the ratio of ether and ketone to sulfonic acid groups, for example whether the amount of double-ether units in s-PEEK (E 730) is the reason for the nearly doubled intensity of the main signal with intermediate *g*. An answer to this question requires the identification of the signals.

3.1.3. Suggested Origin of the Signals. According to the chemical structure (Scheme 2), degradation is possible by attack at different positions. The $^{\bullet}$OH radical as a well-known oxidation agent acts as an electrophile. Therefore, positions of high electron density are preferred for radical reaction. Arrows in Scheme 2 show the possible sites of attack.

Electrophilic $^{\bullet}$OH attack at position **a**: The radical adds to the substituted ring carbon and delocalizes its unpaired electron within the π system via formation of a cyclohexadienyl

intermediate. Breaking the ether bond restores the aromatic system on one side and leads to an oxygen centered phenoxy radical at the other fragment. g values around 2.0033 and hyperfine splitting into a multitude of lines with H(1) splittings around 34 G are expected for cyclohexadienyl radicals.[17]

The sulfonic acid group with its pK_a of -2.6 has a strong tendency to dissociation. Therefore, ion pairs will be formed as soon as water in the membrane material allows solvation of the protons. No matter whether $^{\bullet}$OH radicals attack the sulfonic acid groups (**b**) by hydrogen abstraction or at sulfur, the resulting radical will have electron density distributed between the oxygen and sulfur atoms. This detected g value is higher than for pure oxygen centered species, for example 2.007, and supports the proximity to sulfur. Following this (**b**), the sulfur remains attached to the polymer. By radical substitution at position **c**, instead, the sulfonic acid group is expected to dissociate from the polymer, which leads to phenol and a free sulfonic acid radical. The latter is normally washed out and detected in product water.

As elemental analysis does not show any changes in the ratio of carbon to sulfur, the side chain cleavage (**c**) does not seem to take place to an extent that is detectable by this method of limited sensitivity.

$^{\bullet}$OH addition at the planar carbonyl carbon center (**d**) leads to an oxygen centered localized radical in the polymer structure. Further reaction via bond-break forms a carboxylic acid on the one and an α carbon-centered σ phenyl radical on the other side. The acidic end group represents a product of backbone cleavage that is well-known in literature[18] for perfluorinated samples like Nafion.

If radical addition takes place at the ring (**e**), the cyclohexadienyl species (compare **a**) may terminate either via disproportionation or via cross-linking with another chain defect.

Scheme 2. Possible Sites of $^{\bullet}$OH Radical Attack on Sulfonated Poly(ether ketones) (s-PEK)

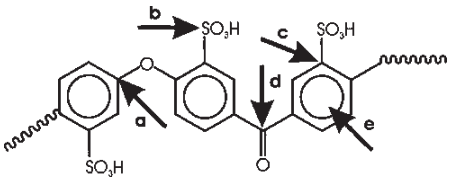

Cyclohexadienyl radicals were so far not detected in the present systems, perhaps due to the multiline hyperfine splitting or also because of too low concentration or too short lifetime, while in earlier EPR experiments with model compounds in aqueous solution they were clearly observed.[19]

The degradation species of poly(2,6-dimethyl-1,4-phenylene oxide) (PPO), which has a structure similar to that of s-PEK, were investigated previously.[20] The results support participation of reactions **a** and **b.** PPO was also proposed as a backbone for polymer membranes in fuel cells.[13] A decay mechanism analogous to the one proposed for PPO is illustrated for s-PEK in Scheme 3.

The polymer main chain consists of an analogous backbone structure of ether-bridged aromatic rings. Ketone groups in s-PEK can give additional EPR signals on oxidative degradation, but their −M (mesomeric electron withdrawing effect through delocalized systems) and −I (inductive electron withdrawing effect through σ bonds) effects are not expected to influence radical formation at ether groups on the remote side of the aromatic ring. Furthermore, the inductive effects of the methyl substituents of PPO (denoted here "side chain") are weak and negligible. In comparison, the sulfonic acid substituents have a dominating +M-effect which stabilizes π radicals. Therefore, with the exception of the sulfur center, the same radicals are expected in s-PEK as in PPO but perhaps in higher concentration because of stabilization.

For PPO a radical driven, photo-oxidative degradation mechanism has been described:[20] A reaction **a**′ similar to **a** (Schemes 2 and 3) was found to represent the main channel. By chain cleavage it leads to phenoxy radicals (poly(2,6-dimethylphenoxy), PDMP) showing a multiplet at g = 2.0049. The line splitting is caused by β hydrogen atoms of neighboring methyl groups, which are absent in s-PEK.

Hence, EPR active phenoxy radicals (PDMP) are formed from PPO. PDMP forms byproduct of yellow color.[21] The darkening of the investigated s-PEK materials is a strong indication for the formation of phenoxy radicals with degradation time. For the more common and better investigated perfluorinated membranes like Nafion, main chain scission has been described.[22] There, radical attack is assumed to occur next to the ether bond[23] which is a preferential position of attack in s-PEK as well.

Scheme 3. Possible Sites of Radical Attack on PPO[20] (Left) and Sulfonated Poly(ether ketones) (Right)

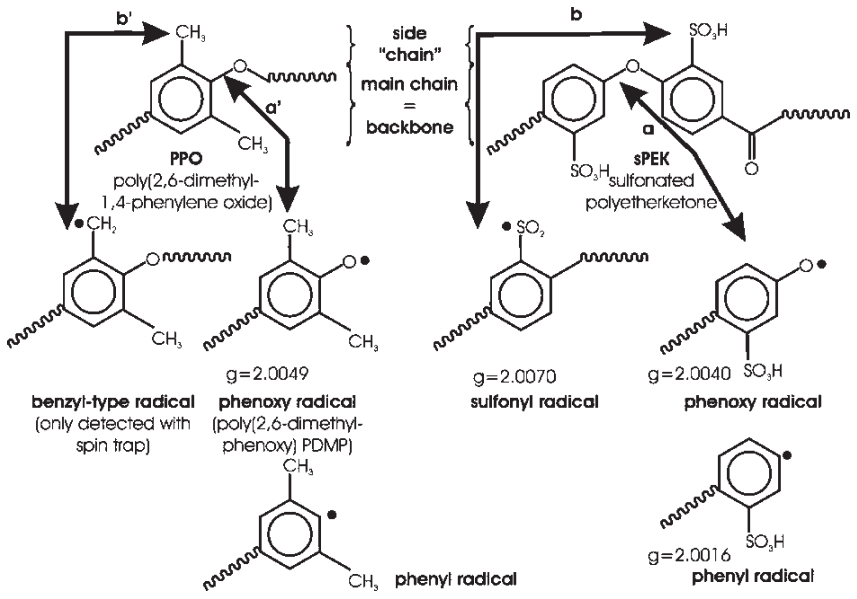

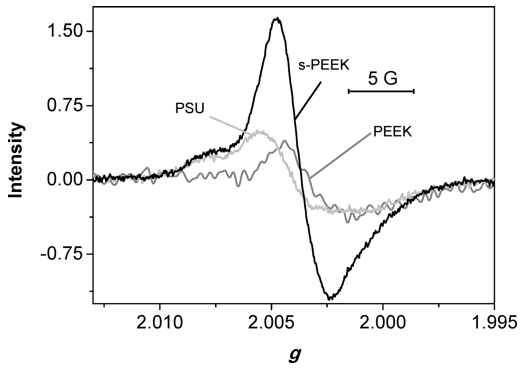

Figure 4. Signals of s-PEEK (E 730, black), sulfonated polyether (PSU, light gray) and PEEK (gray) at 4 mW microwave power and 80 °C.

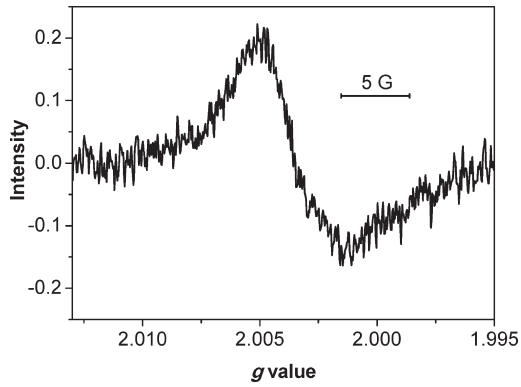

Figure 5. EPR signal of s-PEEK (E 730) after 2 h treatment in dry nitrogen at 80 °C measured at 4 mW.

While PDMP gives a split signal at $g = 2.0049$, the s-PEK phenoxy radical can be assigned to the detected unsplit signal near $g = 2.0036$. In organic π-type radicals, g values higher than g_e generally arise from increased spin−orbit coupling of the electron on heavier atoms. Values >2.0030 indicate some admixture of oxygen orbitals, and 2.0049 is typical for phenoxy radicals.

By the same attack at the ether bond (**a** and **a′** in Scheme 3) the formation of phenyl radicals is suggested. They were not discussed by Scoponi et al.[20] as they were not detected. For s-PEK the lowest g value is assumed to belong to the phenyl radical. Its σ character legitimates the g value of 2.0016 which is lower than that of the free electron.[20]

Other attacks occur at methyl groups ("side chain" of PPO, **b′** in Scheme 3). For PPO the resulting benzyl-type radicals have been verified by the spin trap technique.[20] Assuming formally the same position of attack on the "side chain" (here the sulfonic acid group) of polyetherketones (**b** in Scheme 3) the reaction would occur under formation of sulfonyl ($ArSO_2^{\bullet}$) radicals. Sulfonyl π radicals show strongly structure dependent g values[24,25] in the range between 2.005 and 2.010,[26] which includes also the measured value of 2.0068. It is assumed that the measured signals near $g = 2.007$ are related to sulfur centered radicals derived from sulfonic acid.

It is noted that a recent review on thermal degradation of PEEK membranes[27] also expects the ether and ketone chains to break via formation of phenoxy and phenyl radicals. Pinteala et al.[16] proved this by spin trapping EPR experiments following UV irradiation of hydrogen peroxide in the presence of s-PEEK polymer.

3.1.4. Additional Experiments Supporting Radical Assignment. In support of the above considerations based on literature two further experiments were performed with polymers containing in part the chemical building blocks which are expected to give the EPR signal (see Table 1). PEEK (pellets by Victrex, molten to a film at 400 °C) which unlike s-PEEK (E 730) does not carry any sulfonic acid groups was used to distinguish the existence of sulfur centered radicals. Sulfonated polysulfone-ether (PSU) was chosen because it contains sulfone groups and dimethyl bridges in place of ketone groups. The film thicknesses were similar to those of the membranes (30 μm), but reactions are expected to take place in the outer 2 μm near the surface.[28]

Figure 4 shows the signals of s-PEEK (E 730), PEEK, and PSU. The black line represents the s-PEEK (E 730) spectrum with g values of 2.0070, 2.0036, and 2.0016. The dark gray line for PEEK shows only the lines with g values of 2.0035, 2.0019, while the high-g shoulder is missing. The light gray line of PSU shows again all three lines ($g = 2.0070$, 2.0040, and 2.0012) but the ratio of the intensities is different to that observed with s-PEEK. The line positions of s-PEEK, PEEK and PSU agree roughly, indicating that they belong to the same species.

Assuming that s-PEEK forms carbon centered phenyl ($g = 2.0016$), oxygen centered phenoxy ($g = 2.0036$) and sulfur centered sulfonyl ($g = 2.0070$) radicals, several conclusions for PEEK and PSU can be drawn: (i) The fact that the high-g shoulder is missing in PEEK that does not contain sulfonic acid groups supports that the corresponding signal in s-PEEK is caused by the sulfonic acid group derived sulfur centered degradation products (e.g., $ArSO_2^{\bullet}$ radicals near $g = 2.0070$). (ii) PSU gives nearly the same signal as s-PEEK although it does not contain any carbonyl groups. Therefore, the resonances near $g = 2.0040$ and $g = 2.0016$ must result from the reaction products of ether cleavage which are phenoxy radicals at $g = 2.0040$ and phenyl radicals at $g = 2.0016$. Both are in the same range as observed for s-PEEK. Small deviations are caused by the structural differences in the polymer which influence radical centers via the delocalized π system.

3.2. Time Dependence. *3.2.1. Strain-Induced Degradation.* During EPR investigations it was found that membranes stored under dry conditions at room temperature for some weeks already showed an EPR signal. This is detected without any hydrogen peroxide contact and is thus of lower intensity (compare Figures 1 and 5). The signal disappears immediately after wetting the sample, and also after some hours of oxygen contact.

To clarify this effect, a piece of membrane was kept in demineralized water at room temperature for at least 2 h, taken out, gently wiped and fixed in the reactor at 80 °C. By drying the sample in a flow of nonhumidified nitrogen a signal appeared which saturated with time (Figures 5 and 6). The spectra are very similar to those resulting from degradation in hydrogen peroxide, but the line intensities and therefore the relative concentrations of species are different. The sulfur centered species does not seem to contribute, and the ratio of carbon to oxygen centered radicals is much lower than after reaction with hydrogen peroxide.

The formation of these radical defects is still observed when the sample is treated in slightly humidified nitrogen (1.8% (80 °C) and 3.5% (65 °C) r.h.). Several series of measurements showed that this nonoxidative degradation depends very strongly on the relative humidity, but hardly on temperature. This observation suggests that the radicals arise from chain rupture due to strain arising within the polymer during shrinking. This process has been observed many years ago by stretching polymers in an EPR cavity and measuring resulting defects.[29] In a humid environment, water uptake

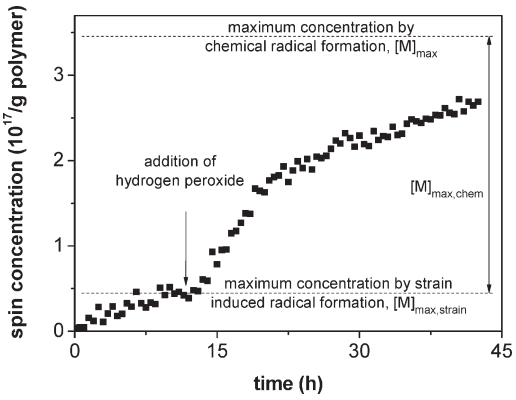

Figure 6. Development of spin concentration [•MOH] on the s-PEEK (E 730) membrane in dry nitrogen followed after 13 h by 3% hydrogen peroxide vapor at 65 °C.

"lubricates" the chains and helps to release the mechanical strain. The fact that the shoulder at $g = 2.0070$ corresponding to sulfonic acid derived radicals is missing is in line with expectation, since the sulfonic acid groups are not influenced by strain in the main chain.

Also Meyer et al.[30] have described such behavior for sulfonated polyimide membranes in a working fuel cell. They suggested two competing degradation mechanisms, oxidation by radicals and a thermally activated process. Higher water contents in the microstructure allow partial recombination of broken polymer chains. Additionally, swelling–deswelling cycles reduced the lifetime of sulfonated polyimide by a factor of 4, while Nafion lost as much as a factor of 200. The ratio of strain induced to chemical reaction induced spin concentration depends on the type of material and on its history. This was described for Nafion by Onishi et al.[7] who found that much misinterpretation occurs when the polymer is insufficiently conditioned before analysis. The hydrophobic PEEK polymers, in contrast, do not show swelling and therefore do not lead to internal strain. However preferred positions for bond rupture on ether and ketone bridges were demonstrated by mass spectrometry.[27] This is another hint for the weakness of these bridges, which obviously break easily either by internal or external forces.

Thus, even though strain induced degradation is not yet completely understood, its contribution to the overall spin concentration on the polymer has to be taken into account.

Figure 6 shows the time dependence of radical signals observed with s-PEEK (E 730) after storage in water. During the first 13 h in a dry nitrogen flow the spin concentration increases up to a saturation value $[M]_{max,strain}$ of about 0.5×10^{17} g^{-1}. Addition of hydrogen peroxide then leads to pronounced increase to a new saturation value $[M]_{max}$, a factor of 3 to 8 higher than $[M]_{max,strain}$.

3.2.2. Chemical Degradation. Radical degradation signals are first observed after about 5 min of hydrogen peroxide treatment, but no mass loss was detectable even after 24 h. Therefore, the sensitivity of EPR is higher by a factor of ≈300 than that of weight loss determination.

Figures 7 and 8 show the signal development with time quantified by fitting the EPR signals and calibration against a spin standard. All measurements were carried out under the same conditions so that the relative errors are close to the lower possible limit of 10%.[31]

Two criteria can be used to analyze a measured curve: (i) the gradient of the spin concentration near time zero represents the initial rate R of radical formation and is a direct measure of the chemical inertness of the polymer. (ii) The maximum spin concentration, $[M]_{max,chem}$, represents the balance between radical formation and termination. These parameters are independent of any detailed kinetic model and obtained qualitatively directly from the measured curves in Figure 7 and 8. Table 3 shows the results for s-PEEK (E 730) and s-PPEK (P 730) at 65 as well as 80 °C.

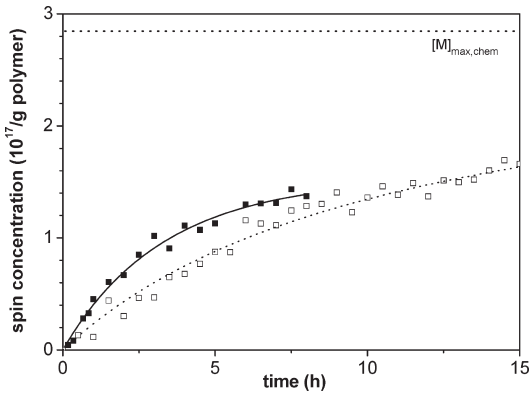

Figure 7. Development of spin concentration [•MOH] obtained with s-PEEK (E 730) at 80 (filled squares) and 65 °C (open squares), using 3% hydrogen peroxide vapor in N_2 at a flow of 0.4 L min^{-1}. The solid curve represents the fit of eq 8, the dotted curve the fit of eq 10, the dotted line at the top the maximum spin concentration $[M]_{max,chem}$.

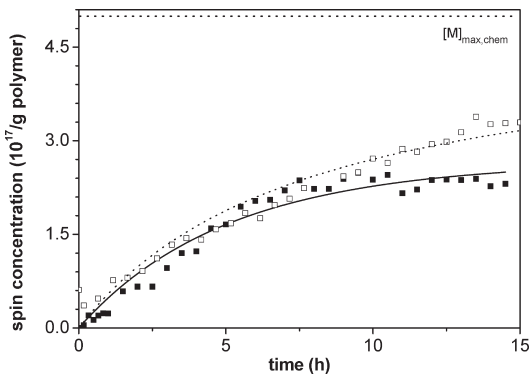

Figure 8. Development of spin concentration [•MOH] obtained with s-PPEK (P 730) in 3% hydrogen peroxide vapor at 80 °C (filled squares) and 65 °C (open squares) at a nitrogen flow of 0.4 L min^{-1}. The symbols represent the experimental data, the solid curve the fit of eq 8, the dotted curve the fit of eq 10. The dotted line on the top represents the maximum spin concentration $[M]_{max,chem}$.

Table 3. Initial Rate R of Radical Formation and Maximum Spin Concentration Observed with s PEEK (E 730) and s-PPEK (P 730) (Estimated Without Fitting from Figures 7 and 8)

sample	T/°C	$[M]_{max,chem}/10^{17}$ spins g^{-1}	$R/10^{16}$ spins g$^{-1}\cdot$h^{-1}
P 730	80	1.7	3.4
	65	2.8	4.0
E 730	80	2.4	4.0
	65	4.9	2.0

The values show that the rates of radical formation are close to a factor two larger for E 730 at 65 °C, and in the same range at 80 °C, thus P 730 appears to be chemically more inert. Furthermore, the saturation spin concentration $[M]_{max,chem}$ of both samples is lower at 80 °C than at 65 °C, although saturation is not reached in the experiments so that these numbers have a large error. While this qualitative evaluation is quick and its interpretation straightforward it is desirable to find an accurate fitting expression for a safer and more detailed interpretation. This is undertaken in the following paragraph.

3.2.3. Development of a Kinetic Model. We start with a historic mechanism where the behavior of hydrogen peroxide on surfaces, also those of polymers, was described by a dissociative Langmuir mechanism[32] (Scheme 4a, eq 2):

$$\begin{aligned} &\mathrm{HO-OH_{gas}} + \mathrm{M} + \mathrm{M} \underset{k_{-1}}{\overset{k_1}{\rightleftharpoons}} \mathrm{HO-OH_{ads,1M}} + \mathrm{M} \underset{k_{-2}}{\overset{k_2}{\rightleftharpoons}} \\ &\mathrm{HO-OH_{ads,2M}} \underset{k_{-3}}{\overset{k_3}{\rightleftharpoons}} 2\,{}^{\bullet}\mathrm{MOH} \xrightarrow{k_{\mathrm{Rec.}}} \mathrm{P_{dia}} \end{aligned} \tag{2}$$

A hydrogen peroxide molecule from the vapor ($HO-OH_{gas}$) adsorbs on the membrane, occupying at first one free site at the membrane surface (k_1). Since the interaction is weak, the molecule can redesorb (k_{-1}). Adsorption is completed as soon as the second oxygen atom of the peroxide succeeds in finding a second membrane binding site ($HO-OH_{ads,2M}$) for adsorption (k_2, k_{-2}). This double adsorption weakens the peroxide bond and promotes homolytic bond cleavage (k_3) of the peroxide (Scheme 4a, eq 2). Thereby, a pair of membrane-bound EPR active species ${}^{\bullet}MOH$ is formed. Termination of radical species is possible either by back reaction (k_{-3}) or by recombination or disproportionation of two neighboring radicals (k_4).

This model involves seven rate constants and the concentrations of various reactant, intermediate and product species. Considering that a single species is observed as a function of time it is impossible to solve for all unknowns. This calls for rigorous simplifications, which are described in the following.

When the radical mobility on the surface is high enough, radicals can terminate by recombination or disproportionation to diamagnetic products (P_{dia}, Scheme 4b). This becomes important only when the surface is almost fully covered,[32] and it is neglected in the present context as the degree of coverage is quite low (compare calculation in section 3.2.5). Radical termination is taken into account by the last term of eq 2. The overall reaction is described by the following differential equations:

$$\frac{\mathrm{d}[\mathrm{HO-OH}]_{\mathrm{gas}}}{\mathrm{d}t} = -k_1[\mathrm{HO-OH}]_{\mathrm{gas}}[\mathrm{M}] + k_{-1}[\mathrm{HO-OH}]_{\mathrm{ads,1M}} \tag{3}$$

$$\frac{\mathrm{d}[\mathrm{HO-OH}]_{\mathrm{ads,1M}}}{\mathrm{d}t} = k_1[\mathrm{HO-OH}]_{\mathrm{gas}}[\mathrm{M}] - k_{-1}[\mathrm{HO-OH}]_{\mathrm{ads,1M}} - k_2[\mathrm{HO-OH}]_{\mathrm{ads,1M}}[\mathrm{M}] + k_{-2}[\mathrm{HO-OH}]_{\mathrm{ads,2M}} \tag{4}$$

$$\frac{\mathrm{d}[{}^{\bullet}\mathrm{MOH}]}{\mathrm{d}t} = 2k_3[\mathrm{H_2O_2}]_{\mathrm{ads,2M}} - 2(k_{-3} + k_4)[{}^{\bullet}\mathrm{MOH}]^2 \tag{5}$$

Since hydrogen peroxide is replenished permanently by the gas flow its concentration is constant, and $d[HO-OH]_{gas}/dt = 0$.

The rates of the partial reactions 3 and 5 depend on the concentration of unoccupied membrane sites [M]. For chemisorption according to the Langmuir model this concentration is given by the maximum concentration of free membrane sites, $[M]_{max}$, reduced by the concentration of surface radicals, $[{}^{\bullet}MOH]$. Therefore, [M] is given by $[M] = [M]_{max,chem} - [{}^{\bullet}MOH]$ and its derivative is $d[M]/dt = -d[{}^{\bullet}MOH]/dt$.

Scheme 4. Suggested Reaction Pathway between Hydrogen Peroxide and Membrane Surface: (a) Adsorption Equilibrium and Hydrogen Peroxide Dissociation; (b) Radical Termination

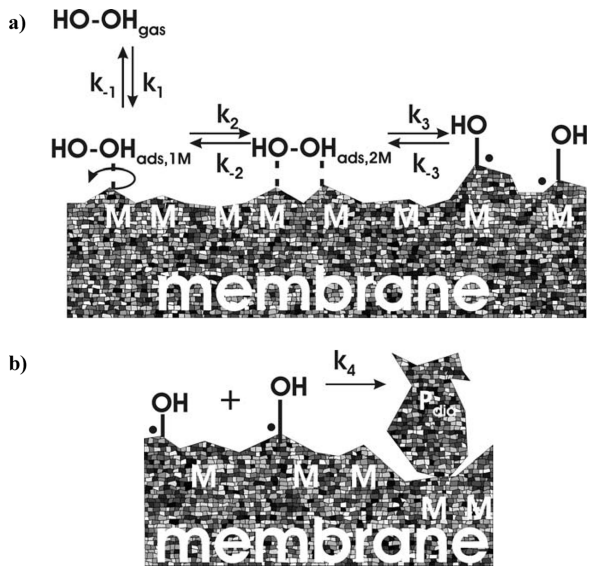

As long as only $[{}^{\bullet}MOH]$ is observed, the back reaction (represented by k_{-3}), and termination (represented by k_4) are kinetically indistinguishable. We therefore subsume both processes in k_T. With these considerations, eqs 3 and 5 become

$$\frac{\mathrm{d}[{}^{\bullet}\mathrm{MOH}]}{\mathrm{d}t} = k_{\mathrm{tot}}([\mathrm{M}]_{\mathrm{max,chem}} - [{}^{\bullet}\mathrm{MOH}])^2 - 2k_{\mathrm{T}}[{}^{\bullet}\mathrm{MOH}]^2 \tag{6}$$

with

$$k_{\mathrm{tot}} = \frac{2k_1k_2k_3[\mathrm{H_2O_2}]_{gas}}{2k_1k_3[\mathrm{H_2O_2}]_{gas} + k_{-1}k_{-2}} \tag{7}$$

Solving this differential equation for the boundary condition $[{}^{\bullet}MOH]_{t=0} = 0$ gives

$$[{}^{\bullet}\mathrm{MOH}] = \frac{k_{\mathrm{tot}}[\mathrm{M}]_{\mathrm{max,chem}}{}^2(\exp[2\Omega t] - 1)}{k_{\mathrm{tot}}[\mathrm{M}]_{\mathrm{max,chem}}(\exp[2\Omega t] - 1) + \frac{\Omega}{2}(\exp[2\Omega t] + 1)} \tag{8}$$

with

$$\Omega = \pm 2[\mathrm{M}]_{\mathrm{max,chem}}\sqrt{k_{\mathrm{tot}}k_{\mathrm{T}}} \tag{9}$$

Only the positive values of Ω are physically relevant. For $k_T = 0$, eq 8 becomes trivial ($[{}^{\bullet}MOH] = 0$), and in the limit of $k_T \rightarrow 0$ eq 8 simplifies to

$$[{}^{\bullet}\mathrm{MOH}] = \frac{[\mathrm{M}]_{\mathrm{max,chem}}t}{t + \frac{1}{2k_{\mathrm{tot}}[\mathrm{M}]_{\mathrm{max,chem}}}} \tag{10}$$

$[M]_{max,chem}$ is the total number of sites for radical attack at the membrane surface. Assuming that the material is homogeneous its value is characteristic and therefore fixed for one batch of membrane. $[{}^{\bullet}MOH]$ equals the observed spin concentration at time t of hydrogen peroxide treatment.

Table 4. Results of Fits of Eqs 8 and 10 to the Time Dependent Spin Concentrations of s-PEEK (E 730) and s-PPEK (P 730)

sample	T/°C	$[M]_{max,strain}/10^{16}$ spins g^{-1}	$[M]_{max,chem}/10^{16}$ spins g^{-1}	$k_{tot}/10^{-19}$ g $spin^{-1}$ h^{-1}	$k_T/10^{-19}$ g $spin^{-1}$ h^{-1}	$2k_{tot}[M]^2_{max,chem}/10^{16}$ spins $g^{-1}\cdot h^{-1}$
P 730	80	6.1 ± 0.3	48 (fix)	1.2 ± 0.1	0.7 ± 0.2	5.4 ± 0.3
	65	10.3 ± 1.4	48 ± 1	1.3 ± 0.2	$\rightarrow 0$	6.2 ± 0.8
E 730	80	2.3 ± 0.9	29 (fix)	2.9 ± 0.1	2.1 ± 0.5	4.7 ± 0.2
	65	8.6 ± 1.9	29 ± 1	1.6 ± 0.1	$\rightarrow 0$	2.5 ± 0.2

Fitting eq 8 to the data sets leads to the following behavior: For the measurements at 65 °C, the termination rate k_T tends toward zero. This means that no recombination occurs, and therefore eq 10 can be applied. The saturation behavior of the kinetic curves at $[M]_{max,chem}$ is in this case given solely by the Langmuir kinetics. For the measurements at 80 °C k_T is not close to zero. It is therefore necessary to use eq 8 which contains one parameter more than eq 10. The parameters, particularly k_T and $[M]_{max,chem}$, are highly correlated and therefore imprecise. As per definition $[M]_{max,chem}$ is constant for a given type of membrane, its value was taken from the 65 °C data. This allows the remaining variables (k_{tot} and k_T) to become more precise.

The gradient of eq 8 at $t \rightarrow 0$ is given by $2 \cdot k_{tot} \cdot [M]^2_{max,chem}$. It represents the rate of radical formation at time zero (R in Table 3), which is a good parameter to judge the membrane inertness against radical attack.

The introduced kinetic model is based on the Langmuir description, which results in the square dependence in eq 6. Another model which has no restriction on available reaction sites at the surface was also applied but matches the curvature of experimental data significantly less well. This may be taken as first evidence that the Langmuir model is correct. Nevertheless, several uncertainties remain. In particular, it is not possible to determine separately all parameters contained in k_{tot}. This is a consequence of the fact that [•MOH] is the only observable quantity. The fit results for the two membranes are given in Table 4.

3.2.4. Ratio of Strain Induced Degradation to Chemical Degradation. The maximum spin concentration generated by strain induced degradation ($[M]_{max,strain}$) is a factor of 3−12 lower than the one caused by degradation with hydrogen peroxide ($[M]_{max,chem}$). This factor is expected to depend on the material under investigation and on humidity.

By increasing the temperature from 65 to 80 °C, the number of strain induced radicals, ($[M]_{max,strain}$), is reduced by a factor of 2 for s-PPEK (P 730) and by a factor of 3 for s-PEEK (E 730). Explanations for this behavior consist in different strain built up in the polymer chains. The two polymers vary in their glass transition temperature by roughly 70 °C (Table 1[11]). As this parameter increases with higher molecular weight (compare Table 1) and reduced mobility of the polymer[33] it can be concluded that there is enhanced sterical strain for s-PPEK (P 730) with its planar, rigid phtalazinone bridge. Higher temperature and therefore smaller relative humidity at the same composition of the treatment gas cause shrinking of the polymer and support chain cleavage. For E 730 the chain tension is expected to be lower than for P 730 because of higher flexibility and possibility for chain reorientation. Therefore, the influence of relative humidity is stronger for this material.

In general the spin concentrations for s-PPEK (P 730) are higher than for s-PEEK (E 730). In relation to the investigations by Meyer et al.[30] the activation energy for "thermal degradation" of polyimide depends on the degree of sulfonation. This is obviously also valid for polyetherketones. So the higher degree of sulfonation of P 730 with an EW of 680 leads to a stronger influence of humidity than for E 730 (EW 820).

3.2.5. Influence of Temperature on the Radical Formation and Termination. Lowering the temperature of s-PEEK (E 730) from 80 to 65 °C decreases k_{tot} by almost a factor of 2. According to the assumptions in section 2.2 the equilibrium constants k_1/k_{-1} and k_2/k_{-2} have an opposite temperature dependence. So the dominating parameter responsible for a decrease of k_{tot} is k_3. Since k_3 changes by more than a factor of 2 (between 65 and 80 °C) it is concluded, that for s-PEEK (E 730) there has to be a small activation barrier for attack. For s-PPEK (P 730) in contrast, changing the temperature has no significant impact on k_{tot}. Therefore, the activation barrier for radical attack on this membrane must be significantly smaller.

$[M]_{max,chem}$ is about two times higher for s-PPEK (P 730) than for s-PEEK (E 730). $[M]_{max,chem.} = 2.8 \times 10^{17}$ spins g^{-1} for s-PPEK. With a mass of about 7 mg per sample and a sample size of about 0.4×3 cm^2 with both sides accessible to radicals, 0.8×10^{15} spins are formed per square centimeter or 8 spins per square nanometer in average for s-PEEK (E 730) and 14 spins for s-PPEK (P 730). It is interesting to see that these numbers are of the same order as literature values obtained after cutting polymers (10^{13} spins$\cdot cm^{-2}$, for polyethylene terephthalate[34] and 10^{15} spins$\cdot cm^{-2}$, for high density polyethylene[35]). This demonstrates that the polymer surface saturates with radical defects, which is further qualitative support for the Langmuir mechanism on which the present kinetic model is based.

k_T, the recombination rate, is expected to be smaller at lower temperature. At 65 °C it is close to zero for both membranes. At 80 °C k_T is three times higher for s-PEEK (E 730) than for s-PPEK (P 730). The recombination rate is probably lower for s-PPEK (P 730) because it contains the rigid phtalazinone bridge, which reduces flexibility in the chains and therefore inhibits recombination in general.

At 65 °C, the radical formation rate $2k_{tot}[M]^2_{max,chem}$ of s-PEEK (E 730) is about half of that of s-PPEK (P 730). Since at this temperature the recombination rate is close to zero we conclude that at low temperatures s-PEEK (E 730) is more stable against radical attack than s-PPEK (P 730).

At elevated temperatures the radical formation rates of the two membrane types reach similar values, but the radical termination is three times faster for s-PEEK (E 730). The saturation value, $[M]_{max,chem.}$, is therefore lower. The diamagnetic product is expected to be cross-linked and brittle, and will cause peeling-off the membrane surface slowly. In mass loss experiments, despite equal reactivity to hydrogen peroxide, s-PEEK (E 730) loses its weight faster than s-PPEK (P 730). This demonstrates that criteria other than chemical inertness toward initial radical attack play a role.

3.2.6. Long-Term Experiments. In a long-term experiment, the degradation behavior of a piece of the s-PPEK (P 730) membrane was measured every 30 min for 1 week around the clock. The result is shown in Figure 9. The initial increase during the first 14 h (regime I) does not quite reach the extrapolated saturation value $[M]_{max}$ reported in Table 4. It is followed by two sharp discontinuities (regime II) and for $t > 40$ h a somewhat wavy near-exponential decay (regime III) with a decay constant of (50 ± 3) h^{-1}. The formation of yellowish products is observed as darkening of the

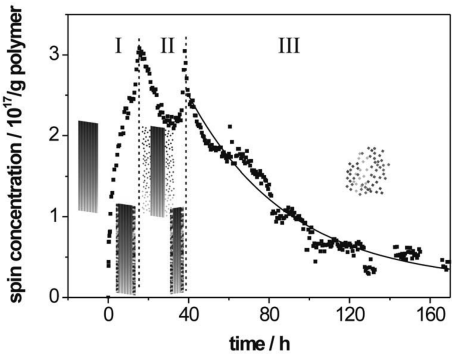

Figure 9. Development of spin concentration on the s-PPEK (P 730) membrane at 80 °C (1.8% r.h. of 3% hydrogen peroxide vapor) and their exponential decay after 60 h. The inset sketches visualize the peel-off effect of the layered membrane: The initial surface ($t < 0$) weakens (0−15 h), membrane pieces leave the material (15−30 h), expose the next layer for attack (30−40 h) up to complete disintegration (40−170 h).

membrane samples. The initial mass of the sample (6.5 mg) was reduced to < 1 mg during the treatment. The weight loss factor coincides roughly with the loss in spin concentration, suggesting that the observed discontinuities represent sudden mass loss. Such behavior is conceivable, considering that radical termination after radical attack leads to cross-linking and therefore to increasing brittleness and peeling-off of the damaged surface layer in pieces. The process may be analogous to skin peeling following heavy sunburn (which is also the consequence of a free radical process at a surface). The overall observed degradation process is always the same, but the time when the peeling process begins is to some extent random. The general behavior is in good agreement with literature where the degradation of nonsulfonated polyethers shows the same behavior.[36]

4. Summary and Concluding Remarks

A setup to measure accelerated degradation of polymer electrolyte membranes was developed. It allows achieving more accurate results a factor of 300 faster than by the traditional mass loss investigations. The higher reproducibility within and the better comparability among the series provides a deeper insight into degradation of the commercially available sulfonated polyetherketones with different ether to ketone ratios (s-PEEK and s-PPEK). Basically the same three radical species, sulfonyl, phenyl and phenoxy radicals were identified for both membranes under all measurement conditions. Their relative abundance depends on the sample and changes with time.

Quantitatively, it was shown that drying the membrane without oxidizing reactants leads to radical defects on the membrane in somewhat lower concentrations. Using hydrogen peroxide to initiate the attack of $^{\bullet}$OH radicals gave rise to radical concentrations larger by factors of 3 to 12 than from drying. The time dependent concentrations can be directly interpreted model-free. Alternatively, a kinetic model allows fitting the data. It suggests that radical formation is not driven by thermal, homolytic bond cleavage of hydrogen peroxide followed by the reaction of $^{\bullet}$OH with the ionomer as often described. Rather, the interaction of the peroxide molecule with the membrane surface is the driving force for bond cleavage in a dissociative Langmuir mechanism. ΔG^0 of thermally activated hydrogen peroxide cleavage in the gas phase is 163 kJ·mol^{-1} at 80 °C (standard concentration: 1 atm).[4] The corresponding equilibrium constant is in the range of 7×10^{-25}, and the equilibrium concentration of hydroxyl radicals approximately 2.7×10^8 spins·L^{-3} under the conditions in the reactor. At the experimental gas flux of 0.4 L min^{-1} 7×10^9 $^{\bullet}$OH radicals pass by the membrane sample per hour. Under the assumption that they all react with the 10 mg membrane this would lead to a radical formation rate R of 7×10^{11} spins g^{-1}h^{-1}, 5 orders of magnitude less than the experimentally observed rate. Thus, even under this optimistic assumption thermal hydrogen peroxide dissociation is not able to explain the radical formation rate. On the other hand, the same gas flux transports 3.3×10^{20} peroxide molecules per hour, more than enough to take care of the experimental radical formation rate of R of 4×10^{16} spins g^{-1}h^{-1}, suggesting again that indeed the Langmuir mechanism of dissociative hydrogen peroxide adsorption is responsible for degradation.

Danilczuk et al. demonstrated the formation of hydroperoxyl radicals in a working fuel cell.[3] In the absence of a Fenton reagent nonthermal hydrogen peroxide cleavage requires the $^{\bullet}$OH trapping energy as a driving force. Unlike perfluorinated polymers, the polyaromatic compounds are highly efficient radical traps. Therefore, the hydroxyl radicals are not available for reaction with hydrogen peroxide to form $^{\bullet}$OOH to any significant extent, and they need not be considered here. Furthermore, their reactivity is much lower than that of $^{\bullet}$OH.[3]

With progressing degradation time, radical formation and recombination weaken the ionomer material. Outer layers break away randomly in pieces, giving way for new attacks (sunburn-like peel-off effect).

Among the two specific studied polymers, s-PPEK has the lower ether content and the higher packing density than s-PEEK, which lowers chain mobility in the polymer. So radical formation is faster, the maximum concentration of radical defects is higher and recombination is hindered. The products of radical termination make the material brittle, force the peeling-off, and are only roughly accessible via mass loss measurements. s-PPEK is the more stable material, although the radical formation rate and the radical concentration are higher.

No radical defects have been detected by this method so far for Nafion or any other perfluorinated membrane material. This is puzzling, since there can be no doubt that Nafion degrades, and a radical mechanism very close to that inferred here for polyaromatic membranes is normally assumed. The ether bridges in Nafion were found to be preferentially broken,[23] fragmentation of the main chain was found several times for example by chromatographic product analysis[37] or loss of molecular weight.[18] Even evidence for the cross-linking to O−S−O was found by infrared spectroscopy for perfluorinated samples.[5] However, ex-situ EPR investigations on Nafion degradation have never shown any evidence of radical formation in the absence of UV light. At this point of investigation the reasons are not clear: either Nafion follows a nonradical degradation pathway, for example because of its much higher hydrophobicity compared to hydrocarbon materials, or the lifetime of radical intermediates is too short for detection.

Transferring these results to real fuel cell conditions needs some additional comments: (i) Formation of hydrogen peroxide in a working fuel cell was already demonstrated some years ago by cyclic voltammetry[38] and recently found to proceed "in a wavelike manner"[39] which is well compatible with the peel-off oscillations found in the present work. However, there is disagreement about whether the peroxide is formed at the cathode (as an intermediate of oxygen reduction) or the anode side (by oxygen crossover). Alternatively, $^{\bullet}$OH and $^{\bullet}$OOH radicals which are also intermediates of oxygen reduction may detach from the catalyst before complete reduction. (ii) There is no catalyst present under the conditions of the present study. This excludes possible complications, since Pt normally tends to induce decomposition of the peroxide. (iii) The influence of UV light which is absorbed by the polymer and can potentially cause photolytic cleavage is excluded as well. (iv) Another aspect to consider is the humidity, which is normally much larger in fuel cells than under

the conditions of this work. There is general agreement that dry conditions accelerate degradation. The advantage of the present study is that such complications are avoided so that the reaction of the polymer can be studied separately.

Acknowledgment. Our special thanks go to Werner Hopf, Thomas Weigend, and Walter Ottmüller for creative, fast, and accurate work in the workshops. We also thank the analysis department of the University of Stuttgart for elemental analysis. Synthesis of PSU samples by Katica Krajinovic of the Institute of Chemical Engineering, University of Stuttgart, is appreciated.

References and Notes

(1) Aleksandrova, E.; Hiesgen, R.; Friedrich, K. A.; Roduner, E. *Phys. Chem. Chem. Phys.* **2007**, *9*, 2735–2743.
(2) Panchenko, A.; Dilger, H.; Kerres, J.; Hein, M.; Ullrich, A.; Kaz, T.; Roduner, E. *Phys. Chem. Chem. Phys.* **2004**, *6*, 2891–2894.
(3) Danilczuk, M.; Coms, F. D.; Schlick, S. *J. Phys. Chem. B* **2009**, *113*, 8031–8042.
(4) Hydrogen Peroxide. In *Gmelin. Handbook of Inorganic Chemistry*; Fluck, E., Ed.; VCH: Weinheim, Germany, 1966; p 2264.
(5) Qiao, J.; Saito, M.; Hayamizu, K.; Okada, T. *J. Electrochem. Soc.* **2006**, *153*, A967–A974.
(6) Aoki, M.; Uchida, H.; Watanabe, M. *Electrochem. Commun.* **2006**, *8*, 1509–1513.
(7) Onishi, L. M.; Prausnitz, J. M.; Newman, J. *J. Phys. Chem. B* **2007**, *111*, 10166–10173.
(8) Zhou, C.; Guerra, M. A.; Qiu, Z. M.; Zawodzinski, T. A.; Schiraldi, D. A. *Macromolecules* **2007**, *40*, 8695–8707.
(9) Mitov, S.; Hübner, G.; Brack, H. P.; Scherer, G. G.; Roduner, E. *J. Polym. Sci., Polym. Phys.* **2006**, *44*, 3323–3336.
(10) Weil, J. A.; Bolton, J. R.; Wertz, J. E., *Principles of Electron Paramagnetic Resonance: Elementary Theory and Practical Applications*, 1st ed.; John Wiley & Sons Ltd.: Chichester, England, 1994.
(11) Bauer, B. Material Safety Data Sheets: E 370 and P 730. www.fumatech.com.
(12) Schuster, M., Personal communication: Sulfonated Hydrocarbon Membranes made by FUMATECH, **2008**.
(13) Ramya, K.; Dhathathreyan, K. S. *J. Appl. Polym. Sci.* **2003**, *88*, 307–311.
(14) Brun, R.; Rademakers, F. *Nucl. Inst. Methods Phys. Res. A* **1997**, *389*, 81–86.
(15) Yang, C. P. *Origin*, 8.0 Pro; OriginLab Corporation: Northampton, MA, 2008.
(16) Pinteala, M.; Schlick, S. *Polym. Degrad. Stab.* **2009**, *94*, 1779–1787.
(17) Taniguchi, H.; Schuler, R. H. *J. Phys. Chem.* **1985**, *89*, 3095–3101.
(18) Hommura, S.; Kawahara, K.; Shimohira, T.; Teraokab, Y. *J. Electrochem. Soc.* **2008**, *155*, A29–A33.
(19) Hübner, G.; Roduner, E. *J. Mater. Chem.* **1999**, *9*, 409–418.
(20) Scoponi, M.; Ghigliorre, C. *Angew. Makromol. Chem.* **1997**, *252*, 237–256.
(21) Slama, Z. *Acta Polym.* **1980**, *32*, 446–451.
(22) Wu, J.; Yuan, X. Z.; Martin, J. J.; Wang, H.; Zhang, J.; Shen, J.; Wu, S.; Merida, W. *J. Power Sources* **2008**, *184*, 104–119.
(23) Ghassemzadeha, L.; Marrony, M.; Barrera, R.; Kreuer, K. D.; Maier, J.; Müller, K. *J. Power Sources* **2009**, *186*, 334–338.
(24) Gilbert, B. C.; Kirk, C. M.; Norman, R. O. C.; Laue, H. A. H. *J. Chem. Soc., Perkin Trans. 2* **1977**, 497–501.
(25) Chatgilialoglu, C.; Gilbert, B. C.; Norman, R. O. C. *J. Chem. Soc., Perkin Trans. 2* **1979**, 770.
(26) Morton, J. R.; Preston, K. F. 1.2.16 Sulfur-centered radicals. In *Landolt-Börnstein - Numerical data and functional relationships in science and technology*; Fischer, H., Ed.; Springer: Berlin, Germany, 1990; Vol. Molecules and Radicals II/17a: Inorganic Radicals, Radical Ions and Radicals in Metal Complexes, pp 97−106.
(27) Patel, P.; Hull, T. R.; McCabe, R. W.; Flath, D.; Grasmeder, J.; Percy, M. *Polym. Degrad. Stab.* **2010**, *95*, 709–718.
(28) Pickett, J. E., Photodegradation and Stabilisation of PPO Resin Blends. In *Mechanisms of Polymer Degradation and Stabilisation*; Scott, G., Ed.; Elsevier: New York, 1990; pp 135−167.
(29) Peterlin, A. *J. Phys. Chem.* **1971**, *75*, 3921–3929.
(30) Meyer, G.; Gebel, G.; Gonon, L.; Capron, P.; Marscaq, D.; Marestin, C.; Mercier, R. *J. Power Sources* **2006**, *157*, 293–301.
(31) Mazur, M. *Anal. Chim. Acta* **2006**, *561*, 1–15.
(32) Satterfield, C. N.; Stein, T. W. *Ind. Eng. Chem.* **1957**, *49*, 1173–1180.
(33) Elias, H.-G., *Macromolecules*; Wiley-VCH: Weinheim, Germany, 2008; Vol. *3*. Physical structures and properties, p 454.
(34) Backman, D. K.; Devries, K. L. *J. Polym. Sci., Polym. Chem.* **1969**, *7*, 2125–2134.
(35) Pazonyi, T.; Tudos, F.; Dimitrov, M. *Angew. Makromol. Chem.* **1970**, *10*, 75–82.
(36) Perrot, C.; Meyer, G.; Gonon, L.; Gebel, G. *Fuel Cells* **2005**, *1*, 10–15.
(37) Carlsson, A.; Joerissen, L. *ECS Trans.* **2009**, *25*, 725–732.
(38) Liu, W.; Zuckerbrod, D. *J. Electrochem. Soc.* **2005**, *152*, A1165–A1170.
(39) Shah, A. A.; Ralph, T. R.; Walsha, F. C. *J. Electrochem. Soc.* **2009**, *156*, B465–B484.